Inorganic Chemistry

Article

pubs.acs.org/IC

Mo-Substituted Keggin Tungstosilicate Microtubes: Preparation and Characterization

Yan Shen,[†] Jun Peng,*[,†] Huanqiu Zhang,[†] Xia Yu,[†] and Alan M. Bond*[,‡]

[†]Key Laboratory of Polyoxometalate Science of Ministry of Education, Faculty of Chemistry, Northeast Normal University, Changchun, Jilin 130024, People's Republic of China

[‡]School of Chemistry, Monash University, Clayton, Victoria 3800, Australia

Supporting Information

ABSTRACT: The synthesis and characterization of microtubes of $SiMoW_{11}$ Keggin polyoxometalates containing either an Mo(V) or Mo(VI) atom is reported. The introduction of a Mo atom into the Keggin-type tungstosilicate microtubes endows them with new properties. The Mo-substituted microtubes may exert both W and Mo functionalities in electrocatalytic reactions and in the immobilization of noble metal nanoparticles. The degree of reduction of the Mo component in the $SiMoW_{11}$ microtubes is controllable simply by tuning the amount of reductant present in the mother liquor. Mo-substituted Keggin tungstosilicate microtubes in their reduced state are more stable than the all-tungsten Keggin tungstosilicate heteropoly blue microtubes.

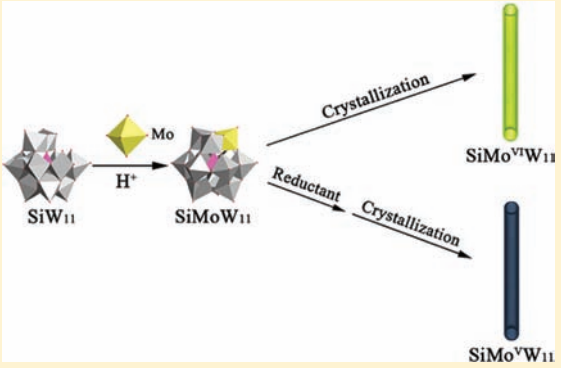

1. INTRODUCTION

Polyoxometalates (POMs), a distinctive class of inorganic metal−oxygen cluster compounds, have attracted much attention because of their wide range of applications in a diverse range of fields.[1] Heteropolytungstates and heteropolymolybdates are of special interest because of their acidic stability and extensive reversible redox chemistry. Importantly, from the perspective of this study, extensive investigations with polyoxotungstates and polyoxomolybdates have indicated that binary mixed-metal POMs may possess enhanced reactivity arising from doping of a second metal component into the POM cluster.[2] This feature has been advantageous in the catalysis of organic oxidation reactions,[3] delignification of wood pulp,[4] fabrication of chemically modified electrodes with electrocatalytic activity,[5] and the efficiency of potential antitumor drugs.[6] Typically, the Keggin-type binary mixed-metal POMs are derived from the reaction of polyoxotungstates or polyoxomolybdates containing a vacant coordination site and the required metal components.

Recently, much effort also has been devoted to the creation of novel materials based on POMs with functional morphology, such as vesicles,[7] honeycombs,[8] and tubes.[9] The fabrication of nano- and microscopic POMs with hollow structures is receiving increasing attention.[10] However, the hollow tubular structure of interest in this study, which is based on binary mixed-metal POMs, has only been rarely reported.

It is known that the monovacant anion $[SiW_{11}O_{39}]^{8-}$ reacts with molybdate in acidic aqueous medium to afford $[SiMoW_{11}O_{40}]^{4-}$ ($SiMoW_{11}$), with the redox behavior[11] being adjusted because of the doping of the second metal Mo. Inspired by this and the above considerations, we have investigated the synthesis of binary mixed-metal POM materials and their reduced forms with tubular structures. In particular, we report the preparations of Mo-monosubstituted Keggin polyoxotungstate microtubes ($SiMo^{VI}W_{11}$) and the corresponding heteropoly blue (HPB) microtubes ($SiMo^{V}W_{11}$), as well as provide a comparative study of the relative redox stabilities of Mo-monosubstituted ($SiMoW_{11}$) and all-tungsten (SiW_{12}) microtubes.[12,13]

2. EXPERIMENTAL DETAILS

2.1. Materials and Methods. $K_8[\alpha\text{-}SiW_{11}O_{39}]$ ($\alpha\text{-}SiW_{11}$) was synthesized according to a published procedure.[14] Na_2MoO_4, Na_2SO_4, H_2SO_4, HCl, and ascorbic acid ($C_6H_8O_6$) were of analytical grade and were used without further purification. All aqueous solutions were prepared with deionized water.

Fourier transform infrared (FT-IR) spectra were recorded with a D/MAX-IIIC spectrometer, X-ray photoelectron spectroscopy (XPS) measurements were undertaken with a Thermo ESCALAB 250 spectrometer combined with an Al Kα (1486.6 eV) achromatic X-ray source, and elemental analysis data were obtained with an Euro Vector EA 3000 instrument. Environmental scanning electron microscopy (ESEM) images were acquired with an XL30 field emission environmental scanning electron microscope (ESEM-FEG). Thermogravimetric (TG) measurements were undertaken with a Perkin-Elmer TGA7 instrument and X-ray diffraction (XRD) analyses with a D/max-IIIC diffractometer. Cyclic voltammograms (CV) were obtained with a CHI 660 electrochemical workstation at room temperature, 20 ± 2°C. A three-electrode system was employed, with a platinum-foil counter electrode, a saturated calomel reference electrode (SCE), and a glassy-carbon working electrode. The POM microtubes were

Received: December 21, 2011
Published: April 23, 2012

   dx.doi.org/10.1021/ic2027412 | *Inorg. Chem.* 2012, 51, 5146−5151

dissolved in 0.25 M Na_2SO_4 + H_2SO_4 solution (pH 1) for electrochemical measurements. Visible spectra were recorded on a 756 CRT ultraviolet/visible spectrometer. Transmission electron microscopy (TEM) and high-resolution transmission electron microscopy (HRTEM) images were acquired with a JEM-2100F microscope with use of an accelerating voltage of 200 kV. The current−voltage (I−V) measurements were obtained with a Keithley 4200 SCS instrument. Fluorescence microscopy images were obtained with an Olympus FV-1000 confocal laser scanning microscope with a mercury lamp as the excitation source, using CCD scanning (objective lens 20 times).

2.2. Preparation of $SiMo^{VI}W_{11}$ Microtubes. α-$K_8[SiW_{11}O_{39}]$ (3 g, 1 mmol) and Na_2MoO_4 (0.2 g, 1 mmol) were placed in a glass beaker having an internally scratched bottom. Water (10 mL) was added with stirring. HCl (3 M) was then added dropwise until the solid dissolved completely and the pH value reached 1, at which point the solution changed from colorless to light yellow. This solution was heated in an 80 °C water bath for 15 min and cooled to room temperature (25 °C) over a period of 10 min. Yellow microtubes of $SiMo^{VI}W_{11}$ rapidly crystallized and were harvested by filtration and dried in air (yield 1.5 g). Anal. Calcd for $SiMo^{VI}W_{11}$ microtubes: K, 4.93; Na, 0.15; Si, 0.93; W, 67.15; Mo, 3.19. Found: K, 4.86; Na, 0.20; Si, 0.89; W, 67.29; Mo, 3.11.

2.3. Preparation of $SiMo^{V}W_{11}$ Microtubes. $SiMo^{V}W_{11}$ microtube synthesis was as for the first stage of the $SiMo^{V}W_{11}$ procedure, except that after heating in an 80 °C water bath for 15 min, ascorbic acid $C_6H_8O_6$ (AA; 1.2 g, 6.8 mmol) was added. Dark blue microtubes of $SiMo^{V}W_{11}$ crystallized after cooling to room temperature (25 °C) and then standing for about 10 min (yield 1.5 g).

3. RESULTS AND DISCUSSION

3.1. Characterization of the $SiMo^{VI}W_{11}$ Microtubes. An optical micrograph (Figure 1a) shows that the color of

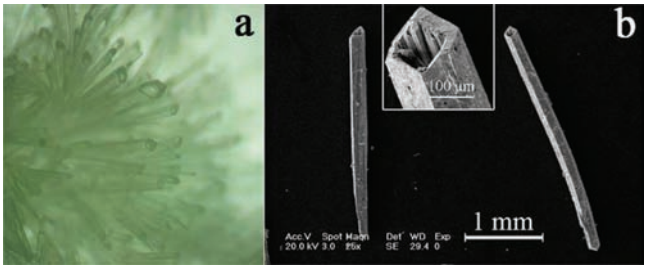

Figure 1. (a) Optical micrograph and (b) ESEM images of $SiMo^{VI}W_{11}$ microtubes.

$SiMo^{VI}W_{11}$ microtubes is light yellow. An ESEM-FEG image (Figure 1b) reveals that the length of an $SiMo^{VI}W_{11}$ microtube is around 3 mm, while the inner diameter and wall thickness are in the ranges of 100−180 and 25−50 μm, respectively. An ESEM image obtained from a $SiMo^{VI}W_{11}$ microtube deliberately destroyed proves the hollow structure (Figure S1a, Supporting Information). To further prove the hollow structure, the $SiMo^{VI}W_{11}$ microtubes were filled with fluorescent $[Ru(bpy)_3]Cl_2$ solution through capillary forces (Figure S2).

The FT-IR spectrum of the $SiMo^{VI}W_{11}$ microtubes (Figure S3) contains the characteristic vibration absorption bands expected for a Keggin anion. The bands at 978, 922, 879, and 777 cm^{-1} are respectively assigned to the ν_{as}(W−O_d), ν_{as}(Si-O_a), ν_{as}(W−O_b−W), and ν_{as}(W−O_c−W) vibrations.[15] The FT-IR spectrum indicates that the $SiMo^{VI}W_{11}$ microtubes maintain the saturated Keggin structure associated with SiW_{12} but does not provide specific proof for the presence of Mo.

XPS spectra, derived from $SiMo^{VI}W_{11}$ microtubes, confirmed the valency of W and Mo (Figure S4). The signals at 35.2 eV (W $4f_{7/2}$) and 37.3 eV (W $4f_{5/2}$) can be attributed to W^{VI}. The presence of Mo^{VI} in the microtubes is confirmed by the signals at 232.8 eV (Mo $3d_{5/2}$) and 235.9 eV (Mo $3d_{3/2}$).[16]

TG and elemental analysis were used to confirm the full formula of the $SiMo^{VI}W_{11}$ microtubes. The TG curve obtained for the $SiMo^{VI}W_{11}$ microtubes shows a one-step mass loss of 2.65% at temperatures below 150 °C, which corresponds to the loss of four water molecules (Figure S5). The elemental analysis data were as follows. Anal. Calcd for $K_{3.8}Na_{0.2}SiMo^{VI}W_{11}O_{40}\cdot 4H_2O$: K, 4.93; Na, 0.15; Si, 0.93; W, 67.15; Mo, 3.19. Found: K, 4.86; Na, 0.20; Si, 0.89; W, 67.29; Mo, 3.11. Thus, the formula $K_{3.8}Na_{0.2}SiMo^{VI}W_{11}O_{40}\cdot 4H_2O$ is established for the $SiMo^{VI}W_{11}$ microtubes.

The X-ray diffraction patterns found for $SiMo^{VI}W_{11}$ microtubes (Figure 2) are similar to those found for SiW_{12}

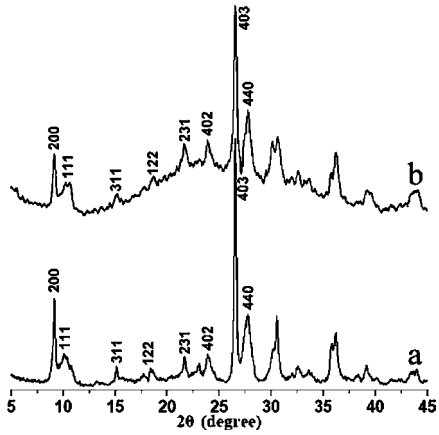

Figure 2. XRD powder patterns obtained from (a) SiW_{12} and (b) $SiMo^{VI}W_{11}$ microtubes.

microtubes,[12] with the latter being attributable to the orthorhombic phase of $K_4SiW_{12}O_{40}$ (JCPDS 70-1714). The HRTEM image clearly reveals lattice fringes with spacings of 0.332 and 0.310 nm attributable to the (403) and (440) crystal faces, respectively (Figure 3). These results verify that the

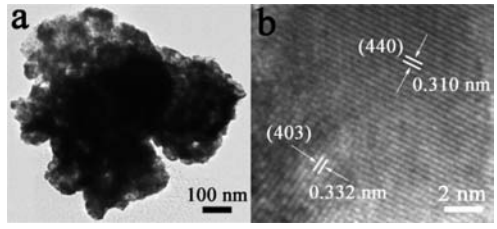

Figure 3. (a) TEM image obtained from a thin section of a $SiMo^{VI}W_{11}$ microtube. (b) HRTEM image derived from a nanoflake of the thin section.

structure of the crystalline saturated Keggin-type POM is maintained in the $SiMo^{VI}W_{11}$ microtubes.

Cyclic voltammetry measurements on a solution of dissolved $SiMo^{VI}W_{11}$ microtubes, along with a control experiment on SiW_{12} microtubes, were carried out under identical conditions to verify the presence of Mo (Figure 4). Three reversible couples, II−II′, III−III′, and IV−IV′, with midpoint potentials, E_m, of −153, −439, and −619 mV found for $SiMo^{VI}W_{11}$

dx.doi.org/10.1021/ic2027412 | Inorg. Chem. 2012, 51, 5146−5151

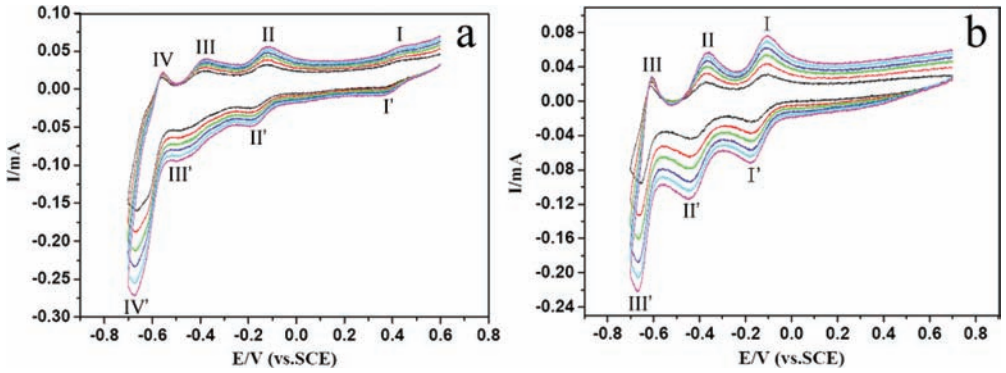

Figure 4. Cyclic voltammograms derived from (a) $SiMo^{VI}W_{11}$ and (b) SiW_{12} dissolved in 0.25 M Na_2SO_4 + H_2SO_4 solution (pH 1) with variable scan rate (from inner to outer: 50, 100, 150, 200, 250, and 300 mV s^{-1}).

microtubes are similar to those of SiW_{12} microtubes but exhibit a slight shift in potentials. The new couple at E_m = 402 mV (I–I′) is ascribed to the electrochemistry of the Mo^{VI}/Mo^{V} redox center, which supports the existence of Mo in the Keggin anion. The introduction of the Mo atom modifies the electrochemical properties of the Keggin tungstosilicate microtubes. This feature is reflected in the fact that the all-tungsten microtubes do not react with the reductant AA in an acidic medium,[13] whereas $SiMo^{VI}W_{11}$ reacts with AA under these conditions. This modified property was used to prepare $SiMo^{V}W_{11}$ microtubes (section 2.3).

3.2. Mechanism for Formation of Mo-Substituted Keggin Tungstosilicate Microtubes. Two obvious reaction routes are available for the formation of Mo-substituted Keggin tungstosilicate microtubes. One requires that the parent α-$K_8[SiW_{11}O_{39}]$ first decomposes to multiple SiW_{12-x} fragments, which in the acidic medium are prone to form saturated α-SiW_{12} and α-$SiMo_xW_{12-x}$ in the presence of W and Mo components. The other is that the parent α-$K_8[SiW_{11}O_{39}]$ reacts stoichiometrically with the Mo component present in the acidic solution. Two experiments were carried out, in which different molar ratios of the starting materials α-$K_8[SiW_{11}O_{39}]$ and Na_2MoO_4 were employed and examined to clarify the nature of the reaction pathway. When the molar ratio of α-$K_8[SiW_{11}O_{39}]$ and Na_2MoO_4 was 1:0.5, the molar ratio W:Mo for the harvested microtubes was 11.4:0.6. When the molar ratio of α-$K_8[SiW_{11}O_{39}]$ and Na_2MoO_4 was 1:1, the molar ratio W:Mo for the harvested microtubes equaled 11:1. These results indicated that the unstable monolacunary Keggin-type polyanion α-SiW_{11} in the acidic medium transformed to the saturated Keggin-type polyanion $[\alpha\text{-}SiMoW_{11}O_{40}]^{4-}$, in the presence of Mo atoms. That is, the Mo atom filled the vacancy available in $SiW_{11}O_{39}^{8-}$ in order to stabilize the structure. This reaction can occur stoichiometrically according to eq 1.[17]

$$[\alpha\text{-}SiW_{11}O_{39}]^{8-} + MoO_4^{2-} + 6H^+ \rightarrow [\alpha\text{-}SiMoW_{11}O_{40}]^{4-} + 3H_2O \quad (1)$$

A previous study on the all-W microtube case showed that the saturated Keggin-type polyanion $[\alpha\text{-}SiW_{12}O_{40}]^{4-}$ initially crystallized as microplanks, which then morphed into the tubular structure.[12] The same mechanism for tube formation would also explain the formation of $SiMo^{VI}W_{11}$ microtubes. That is, the nontubular form of the salt of $[\alpha\text{-}SiMoW_{11}O_{40}]^{4-}$ crystallizes first and then forms a tubular structure.

Analogously, it is believed that the $SiMo^{V}W_{11}$ compound formed through reduction of $[\alpha\text{-}SiMo^{VI}W_{11}O_{40}]^{4-}$ in the presence of AA in the mother liquor (eq 2) forms a salt of $[\alpha\text{-}SiMo^{V}W_{11}O_{40}]^{5-}$, which then crystallizes to form $SiMo^{V}W_{11}$ microtubes.

$$2[\alpha\text{-}SiMo^{VI}W_{11}O_{40}]^{4-} + C_6H_8O_6 \rightarrow 2[\alpha\text{-}SiMo^{V}W_{11}O_{40}]^{5-} + C_6H_6O_6 \quad (2)$$

The mechanism proposed for the formation of the $SiMo^{VI}W_{11}$ and $SiMo^{V}W_{11}$ microtubes is summarized in Scheme1.

Scheme 1. Mechanism Postulated for Formation of $SiMo^{VI}W_{11}$ and $SiMo^{V}W_{11}$ Microtubes

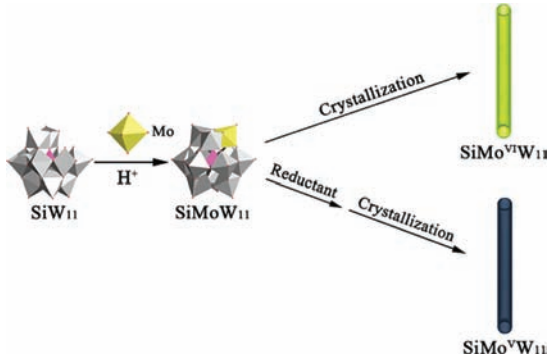

3.3. Characterization of the $SiMo^{V}W_{11}$ Microtubes. An optical micrograph and an ESEM image of $SiMo^{V}W_{11}$ microtubes are shown in Figure 5. The $SiMo^{V}W_{11}$ microtubes are deep blue. The length of the $SiMo^{V}W_{11}$ microtubes is around 1.5 mm. The inner diameter and wall thickness are in the ranges of 20–80 and 10–40 μm, respectively. Similarly, to prove the hollow structures, an ESEM image is taken from a $SiMo^{V}W_{11}$ microtube deliberately destroyed (Figure S1b).

The IR spectrum of the $SiMo^{V}W_{11}$ microtubes is close to that of the $SiMo^{VI}W_{11}$ microtubes, except for two weak bands at 1760 and 1339 cm^{-1}, which are attributed to the carbonyl of the free ester and the enol hydroxy of AA, respectively (Figure S6). This indicates that a trace amount of reductant AA is doped into the $SiMo^{V}W_{11}$ microtubes.[18]

An XPS spectrum was obtained to establish the valency of W and Mo in the $SiMo^{V}W_{11}$ microtubes. The Mo $3d_{5/2}$ and Mo $3d_{3/2}$ signals are located at 232.0 and 235.0 eV, and those of W $4f_{7/2}$ and W $4f_{5/2}$ at 35.9 and 37.8 eV. Significantly, in the

dx.doi.org/10.1021/ic2027412 | Inorg. Chem. 2012, 51, 5146–5151

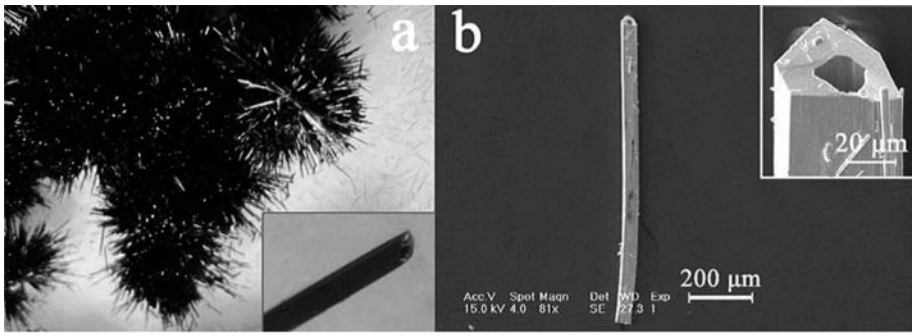

Figure 5. (a) Optical micrographs and (b) ESEM images of the $SiMo^{V}W_{11}$ microtubes.

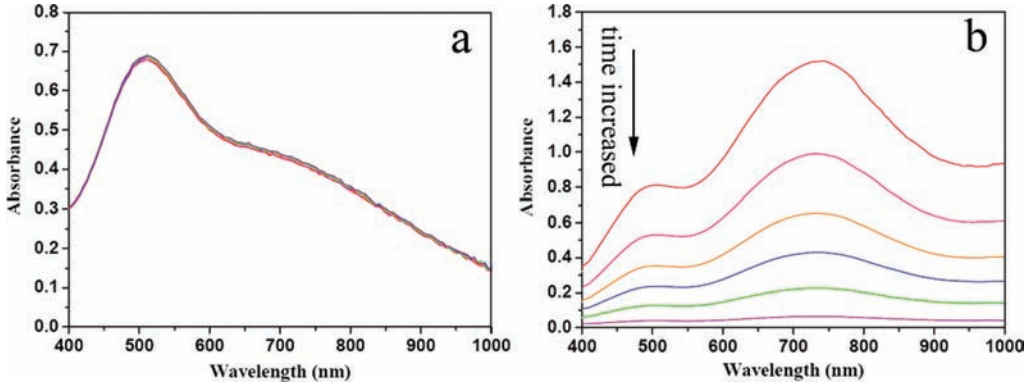

Figure 6. Visible spectra of aqueous solutions of (a) $SiMo^{V}W_{11}$ and (b) SiW_{12}-HPB microtubes recorded every 0.5 h for 2.5 h (from red line to purple line).

$SiMo^{V}W_{11}$ microtubes, all Mo atoms are in the +5 oxidation state, whereas all W atoms are in the +6 oxidation state:[16] that is, W atoms are not reduced by AA in the acidic medium, but Mo atoms can be reduced under the preparation conditions.[13]

The XRD powder pattern for the $SiMo^{V}W_{11}$ microtubes is similar to that for the SiW_{12} microtubes, with only slight differences found in peak positions (Figure S7). Thus, the crystal structure of the saturated Keggin 12-series is maintained intact in the $SiMo^{V}W_{11}$ microtubes, even though substitution of Mo and the presence of AA may slightly disturb the environment.

Solid-state *I*−*V* measurements were undertaken on individual $SiMo^{VI}W_{11}$ and $SiMo^{V}W_{11}$ microtubes. In these measurements, a microtube was placed on a glass substrate and then coated with silver paste on both ends of the microtube to form electrodes. The *I*−*V* curves revealed that the conductivity of a $SiMo^{V}W_{11}$ microtube is higher than that of a $SiMo^{VI}W_{11}$ microtube (Figure S8). This is as expected, as $SiMo^{V}W_{11}$ possesses mobile "blue electrons".

3.4. Stable and Controllable Reduction Properties of $SiMo^{V}W_{11}$ Microtubes. A comparative study on the relative redox stabilities of $SiMo^{V}W_{11}$ and SiW_{12}-HPB microtubes was carried out via control experiments in which 0.5 g of $SiMo^{V}W_{11}$ and SiW_{12}-HPB microtubes was dissolved in 10 mL of water, respectively. The redox levels of the resulting solutions were then monitored by visible spectroscopy every 0.5 h for 2.5 h. The characteristic absorption bands for the intervalence-charge transfer (IVCT) transitions for a Keggin HPB species[19] are centered at ca. 700 nm for a $SiMo^{V}W_{11}$ solution and at ca. 750 nm for an SiW_{12}-HPB solution (Figure 6). After 2.5 h, the intensity of the absorption for the $SiMo^{V}W_{11}$ solution remained unchanged, whereas that for the SiW_{12}-HPB had almost disappeared due to oxidation of $W^{V} \rightarrow W^{VI}$. These results are consistent with the voltammetric data, which showed that $SiMo^{VI}W_{11}$ has a significant positive midpoint potential of E_m = 402 mV (I−I′), whereas these potentials for SiW_{12} in lie in the negative potential range. Thus, it is concluded that $SiMo^{V}W_{11}$ is more stable than SiW_{12}-HPB.

As expected, the rates of the redox reactions for solid $SiMo^{V}W_{11}$ and SiW_{12}-HPB microtubes are much slower than for the corresponding solutions. Thus, when $SiMo^{V}W_{11}$ microtubes were maintained under ambient conditions for half a year, their color did not change (Figure S9). In contrast, the SiW_{12}-HPB microtubes were bleached within 24 h (Figure S10). This fact also supports the conclusion that Mo-substituted Keggin tungstosilicate HPB microtubes are more stable than the all-tungsten Keggin tungstosilicate HPB microtubes, due to the introduction of a Mo component. This enhanced stability allows immobilization of Ag nanoparticles on the $SiMo^{V}W_{11}$ microtubes to be undertaken under ambient conditions without oxidation of the $SiMo^{V}W_{11}$ microtubes occurring by oxygen during the immobilization process.

A series of preparative experiments was also undertaken to find the relationship between the degree of reduction of the $SiMoW_{11}$ microtubes and the quantity of AA starting material. Under the same reaction conditions for the preparation of $SiMo^{V}W_{11}$ microtubes, variable quantities of AA were added to the mother liquor. The as-synthesized microtubes are labeled as $SiMoW_{11}$-*i*, where *i* represents the amount of AA added: *i* = 1, 0.3 g (1.7 mmol); *i* = 2, 0.6 g (3.4 mmol); *i* = 3, 0.9 g (5.1 mmol); *i* = 4, 1.2 g (6.8 mmol). These microtube samples were dissolved in water to obtain 0.03 M solutions. The resulting solutions then were monitored by visible spectroscopy. The

dx.doi.org/10.1021/ic2027412 | *Inorg. Chem.* 2012, 51, 5146−5151

changes in absorption intensities which are related to the reduction degree of the $SiMoW_{11}$-*i* (*i* = 1−4) microtubes (Figure 7) were then monitored.

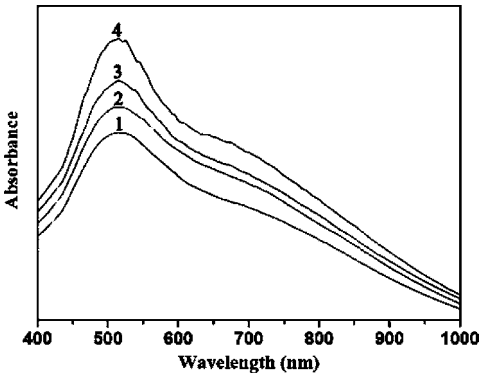

Figure 7. Visible spectra of 0.03 M $SiMoW_{11}$-*i* (*i* = 1−4) solutions, where *i* represents the amount of AA added: *i* = 1, 0.3 g (1.7 mmol); *i* = 2, 0.6 g (3.4 mmol); *i* = 3, 0.9 g (5.1 mmol); *i* = 4, 1.2 g (6.8 mmol).

The visible spectra show that the absorption intensities increase in the order *i* = 1−4. That is, the more AA present in the mother liquor, the higher the degree of reduction of $SiMoW_{11}$ (Figure S11).

XPS analysis also is helpful in determining the degree of reduction of $SiMoW_{11}$-*i* (*i* = 1−4) microtubes (Figures S12 and S13). The existence of Mo^{V} is evidenced by the signal at 231.8 eV. The molar ratio Mo^{V}:Mo^{VI} in $SiMoW_{11}$-i microtubes may be computed from the peak areas of Mo^{VI} ($3d_{5/2}$) and Mo^{V} ($3d_{5/2}$). Table 1 gives the peak area ratios forms for Mo^{V} and Mo^{VI} and the calculated corresponding formula. Furthermore, the W $4f_{7/2}$ and W $4f_{5/2}$ binding energies around 35.8 and 37.8 eV are characteristic of W^{VI} (Figure S13).[16] Clearly, in the $SiMoW_{11}$-4 microtubes, all Mo atoms are present in the +5 oxidation state and W atoms in the +6 oxidation state, which indicates that only the Mo component is reduced in the $SiMoW_{11}$ microtubes under the conditions used for their preparation. Therefore, the degree of reduction of Mo-substituted Keggin tungstosilicate microtubes is tunable and is achieved simply by controlling the amount of AA present in their synthesis.

Table 1. Ratio of Mo^{V} to Mo^{VI} in $SiMoW_{11}$-*i* (*i* = 1−4) Microtubes Obtained from Analysis of XPS Data

sample	ratio of peak area Mo^{V}:Mo^{VI} ($3d_{5/2}$)	ratio of Mo^{VI}:Mo^{V} in $SiMoW_{11}$-*i* microtubes
$SiMoW_{11}$-1	1:0.42	$SiMo^{VI}_{0.3}Mo^{V}_{0.7}W_{11}$
$SiMoW_{11}$-2	1:0.20	$SiMo^{VI}_{0.2}Mo^{V}_{0.8}W_{11}$
$SiMoW_{11}$-3	1:0.11	$SiMo^{VI}_{0.1}Mo^{V}_{0.9}W_{11}$
$SiMoW_{11}$-4	1:0	$SiMo^{V}W_{11}$

4. CONCLUSION

Mo-monosubstituted Keggin tungstosilicate $SiMo^{VI}W_{11}$ and $SiMo^{V}W_{11}$ microtubes have been synthesized. The degree of reduction of the $SiMoW_{11}$ microtubes is linked to the amount of AA in the mother liquor, which is controllable. $SiMo^{V}W_{11}$ microtubes are stable in air, which is favorable for the in situ preparation of metal nanoparticles, for the storage of reductive gases, and for other applications.

■ ASSOCIATED CONTENT

Supporting Information

Figures giving ESEM images of fragments obtained from destroyed $SiMo^{VI}W_{11}$ and $SiMo^{V}W_{11}$ microtubes, fluorescent micrographs of the $SiMo^{VI}W_{11}$ microtubes filled with $[Ru(bpy)_3]Cl_2$, FT-IR spectra of $SiMo^{VI}W_{11}$ and $SiMo^{V}W_{11}$ microtubes, TG data for $SiMo^{VI}W_{11}$ microtubes, XRD powder patterns for $SiMo^{V}W_{11}$ microtubes, XPS spectra (W 4f and Mo 3d) of $SiMo^{VI}W_{11}$ and $SiMoW_{11}$-*i* (*i* = 1−4) microtubes, plots of the peak area ratio of $Mo^{VI}(3d_{5/2})$:$Mo^{V}(3d_{5/2})$ for the $SiMoW_{11}$-*i* (*i* = 1−4) microtubes vs the amount of AA present in the mother liquor, *I*−*V* curves for $SiMo^{VI}W_{11}$ and $SiMo^{V}W_{11}$ microtubes, optical micrographs of $SiMo^{V}W_{11}$ microtubes freshly prepared and maintained under ambient conditions for half a year, and optical micrographs of SiW_{12}-HPB microtubes freshly prepared and exposed to the atmosphere for 24 h. This material is available free of charge via the Internet at http://pubs.acs.org.

■ AUTHOR INFORMATION

Corresponding Author

*E-mail: jpeng@nenu.edu.cn (J.P.); alan.bond@sci.monash.edu.au (A.M.B.).

Notes

The authors declare no competing financial interest.

■ ACKNOWLEDGMENTS

This work was financially supported by the National Natural Science Foundation of China (Grant 21071029), the Fundamental Research Fund for the Central Universities of China, and the Australian Research Council.

■ REFERENCES

(1) (a) Haimov, A.; Cohen, H.; Neumann, R. *J. Am. Chem. Soc.* **2004**, *126*, 11762−11763. (b) Huey, F.; Hargis, L. G. *Anal. Chem.* **1967**, *39*, 125−127. (c) Rhule, J. T.; Hill, C. L.; Judd, D. A. *Chem. Rev.* **1998**, *98*, 327−357. (d) Yamase, T. *Chem. Rev.* **1998**, *98*, 307−325.

(2) (a) Gao, G. G.; Li, F. Y.; Xu, L.; Liu, X. Z.; Yang, Y. Y. *J. Am. Chem. Soc.* **2008**, *130*, 10838−10839. (b) Han, Z. G.; Zhao, Y. L.; Peng, J.; Ma, H. Y.; Liu, Q.; Wang, E. B.; Hu, N. H.; Jia, H. Q. *Eur. J. Inorg. Chem.* **2005**, 264−271.

(3) (a) Hill, C. L. U.S. Patent 4,864,041, 1989. (b) Hill, C. L.; Brown, R. B., Jr. *J. Am. Chem. Soc.* **1986**, *108*, 536−538.

(4) Weinstock, I. A.; Hill, C. L. U.S. Patent 5,302,248, 1994.

(5) Sun, W. L.; Zhang, S.; Liu, H. Z.; Jin, L. T.; Kong, J. L. *Anal. Chim. Acta* **1999**, *388*, 103−110.

(6) Wang, X. H.; Li, J. X.; Yang, Y.; Liu, J. T.; Li, B.; Pope, M. T. *J. Inorg. Biochem.* **2003**, *94*, 279−284.

(7) Li, D.; Zhang, J.; Landskron, K.; Liu, T. B. *J. Am. Chem. Soc.* **2008**, *130*, 4226−4227.

(8) Bu, W. F.; Li, H. L.; Sun, H.; Yin, S. Y.; Wu, L. X. *J. Am. Chem. Soc.* **2005**, *127*, 8016−8017.

(9) Ritchie, C.; Cooper, G. J. T.; Song, Y. F.; Streb, C.; Yin, H. B.; Parenty, A. D. C.; MacLaren, D. A.; Cronin, L. *Nat. Chem.* **2009**, *1*, 47−52.

(10) (a) Kang, Z. H.; Wang, E. B.; Jiang, M.; Lian, S. Y.; Li, Y. G.; Hu, C. W. *Eur. J. Inorg. Chem.* **2003**, 370−376. (b) Ding, B.; Gong, J.; Kim, J.; Shiratori, S. *Nanotechnology* **2005**, *16*, 785−790. (c) Li, J.; Wang, X. H.; Zhu, W. M.; Cao, F. H. *ChemSusChem* **2009**, *2*, 177−183. (d) Cooper, G. J. T.; Boulay, A. G.; Kitson, P. J.; Ritchie, C.; Richmond, C. J.; Thiel, J.; Gabb, D.; Eadie, R.; Long, D. L.; Cronin, L. *J. Am. Chem. Soc.* **2011**, *133*, 5947−5954. (e) Cooper, G. J. T.; Cronin, L. *J. Am. Chem. Soc.* **2009**, *131*, 8368−8369. (f) Gao, J.; Yan, J.; Mitchell, S. G.; Miras, H. N.; Boulay, A. G.; Long, D. L.; Cronin, L. *Chem. Sci.* **2011**, *2*, 1502−1508.

(11) (a) Cui, Y.; Xu, L.; Wang, W. J.; Gao, G. G.; Wang, E. B. *Chin. J. Chem.* **2006**, *24*, 316−320. (b) Kozik, M.; Hammer, C. F.; Baker, L. C. W. *J. Am. Chem. Soc.* **1986**, *108*, 2748−2749.
(12) Xin, Z. F.; Peng, J.; Wang, T.; Xue, B.; Kong, Y. M.; Li, L.; Wang, E. B. *Inorg. Chem.* **2006**, *45*, 8856−8858.
(13) (a) Shen, Y.; Peng, J.; Zhang, H. Q.; Chen, C. Y.; Zhang, F.; Bond, A. M. *J. Mater. Chem.* **2011**, *21*, 6995−6998. (b) Shen, Y.; Peng, J.; Pang, H. J.; Zhang, P. P.; Chen, D.; Chen, C. Y.; Zhang, H. Q.; Meng, C. L.; Su, Z. M. *Chem. Eur. J.* **2011**, *17*, 3657−3662.
(14) Tézé, A.; Hervé, G. *J. Inorg. Nucl. Chem.* **1977**, *39*, 999−1002.
(15) Deltcheff, C. R.; Fournier, M.; Franck, R.; Thouvenot, R. *Inorg. Chem.* **1983**, *22*, 207−216.
(16) Liu, S. H.; Wang, D. H.; Pan, C. H. *Analysis of X-ray Photoelectron Spectroscopy*; Science Press: Beijing, 1988.
(17) Pope, M. T. *Heteropoly and Isopoly Oxometalates*; Springer-Verlag: Berlin, 1983.
(18) Bellamy, L. J. *The Infrared Spectra of Complex Molecules*; Chapman and Hall: London, New York, 1980.
(19) Varga, G. M., Jr.; Papaconstantinou, E.; Pope, M. T. *Inorg. Chem.* **1970**, *9*, 662−667.

dx.doi.org/10.1021/ic2027412 | *Inorg. Chem.* 2012, 51, 5146−5151